remote sensing

Article

Condition Rating of Bridge Decks with Fuzzy Sets Modeling for SF-GPR Surveys

Nicolas Gagarin [1], Dimitrios Goulias [2,*] and James Mekemson [1]

[1] Starodub Inc., Kensington, MD 20895, USA; nicolas.gagarin@starodub.com (N.G.); james.mekemson@starodub.com (J.M.)
[2] Department of Civil and Environmental Engineering, Faculty of Engineering, University of Maryland, College Park, MD 20742, USA
* Correspondence: dgoulias@umd.edu

Abstract: Highway agencies monitor the condition of thousands of bridge decks every year. Even though Ground Penetrating Radar (GPR) has been used in bridge-deck evaluation, Step-Frequency GPR (SF-GPR) provides advanced condition assessment yet requires extensive and complex post-processing analysis. An SF-GPR analysis system was recently developed and used for monitoring the condition of all the bridge decks in the state of Maryland. The objective of this study was to develop a bridge deck condition rating approach using fuzzy sets modeling on the SF-GPR data and analysis. The fuzzy sets membership functions needed to reflect rating score categories similar to those considered in the National Bridge Inventory (NBI) database for uniformity. Thus, the fuzzy sets modeling was built considering nine condition membership functions. The overall bridge deck condition score leading to each of the nine condition states was based on both physical and condition-related bridge deck parameters as obtained from the SF-GPR analysis. The modeling approach is presented herein, along with two bridge deck examples. The proposed novel fuzzy sets modeling can be considered for possible adoption elsewhere where similar GPR systems are used.

Keywords: Step-Frequency Ground Penetrating Radar; condition assessment; bridge decks; fuzzy sets

Citation: Gagarin, N.; Goulias, D.; Mekemson, J. Condition Rating of Bridge Decks with Fuzzy Sets Modeling for SF-GPR Surveys. *Remote Sens.* **2023**, *15*, 3631. https://doi.org/10.3390/rs15143631

Academic Editors: Francesco Soldovieri, Francesco Benedetto, Fabio Tosti, Amir M. Alani, Andreas Loizos and Valerio Gagliardi

Received: 9 May 2023
Revised: 12 July 2023
Accepted: 18 July 2023
Published: 21 July 2023

1. Introduction

There are approximately 615,000 bridges in the United States, with an approximate average age of 51 years. The current estimate for bridge maintenance and rehabilitation of bridges in poor condition in the US is of the order of more than 33 trillion dollars. This represents approximately 68% of the replacement cost [1]. Several billion dollars are spent annually for bridge deck repair and replacement. Concrete bridge decks are designed to provide the necessary structural capacity and surface characteristics with proper friction for safety and smoothness for ride quality. It is the role of infrastructure managers at the national, state, and local levels to maintain bridge decks. A number of non-destructive methods (NDT) have been proposed and used over the years for assessing the condition of concrete bridge decks. These include the simplest methods, such as chain drag, half-cell potential, and visual surveys, to the more advanced methods, including, among others, Ultrasonic and Impact Echo (IE), Thermography (IR), and pulse GPR single antenna or antenna arrays [2–8]. The advantages and limitations of these NDT in terms of speed, accuracy, cost, and required training for the operation and interpretation of data are well documented in the literature [9,10]. In particular, the national study SHRP 2 R06-A, which included a thorough review of NDT methods used for identifying concrete bridge deck deterioration, reached the following important conclusions [11]: a number of NDT technologies can provide detailed and accurate information only about a certain type of deterioration or defect; comprehensive condition assessment of bridge decks can be achieved only through a complementary use of multiple technologies; speed has been a major limitation for most of the technologies, and has been the main obstacle for wide adoption by transportation agencies; and, most of these NDT requires a significant level of training and expertise, especially in data analysis and interpretation. Recent work with ground-coupled impulse GPR for concrete bridge deck condition assessment is documented in various studies [2,3,7,12–14]. Follow-up studies have addressed specific aspects of condition assessment [15–21]. In GPR, short pulses of electromagnetic energy are transmitted into the structure. The reflected waves are received by the antennas and analyzed based on the electromagnetic wave propagation theory [11,13]. Depending on the GPR unit, different frequencies may be used, with low frequencies for higher depth exploration and higher frequencies for shallow depths but higher accuracy [7,14]. For bridge decks, both low and high frequencies are typically needed due to several elements within the bridge deck structure (i.e., cover depth, rebars, below rebar concrete quality, and deck back wall). More recently, GPR data have been analyzed using neural networks for complex infrastructure condition assessment. Examples include pavement crack detection using multiscale feature fusion deep neural networks [22] and convolutional neural networks (R-CNN) for detecting internal small cracks in asphalt pavements at the pixel level [23]. Also, the development of bridge deck rating systems using fuzzy sets analysis has been looked at [24].

Due to the requirements for higher accuracy data for complex structures like bridge decks, the need for SF-GPR has been identified [25,26]. This wideband system versus a traditional single or dual-frequency GPR system is advantageous since it provides an extended series of bandwidth range frequencies covering both the depth and accuracy of complex structures like bridge decks. However, it requires significant and more complex post-processing analysis to deal with the volume of data pertinent to the wide range of reflected signals received from the various frequencies. This often requires the development of specialized algorithms to capture most of the information and accuracy from the reflected signal [27]. Thus, the development and potential use of Step-Frequency Ground Penetrating Radar, SF- GPR, in bridge deck evaluation addresses the limitations of single and/or dual frequency systems [28].

1.1. SF-GPR System & Post-Processing Analysis

Recently an SF-GPR system combined with advanced post-processing algorithms was developed for the state of Maryland and presented previously [28,29]. In the developed system, a 3D-Radar DXG1820 antenna array was used in near-ground conditions. While the 3d Examiner software was available, proprietary software was used since it provided better post-processing data analysis capabilities as defined next [30]. The 1.8 m wideband antenna array has a frequency ranging between 200 MHz–3 GHz, maximizing thus the resolution at each depth level, and with an array of transmitter and receiver antennas, Figure 1, and a scan width of 1.5 m.

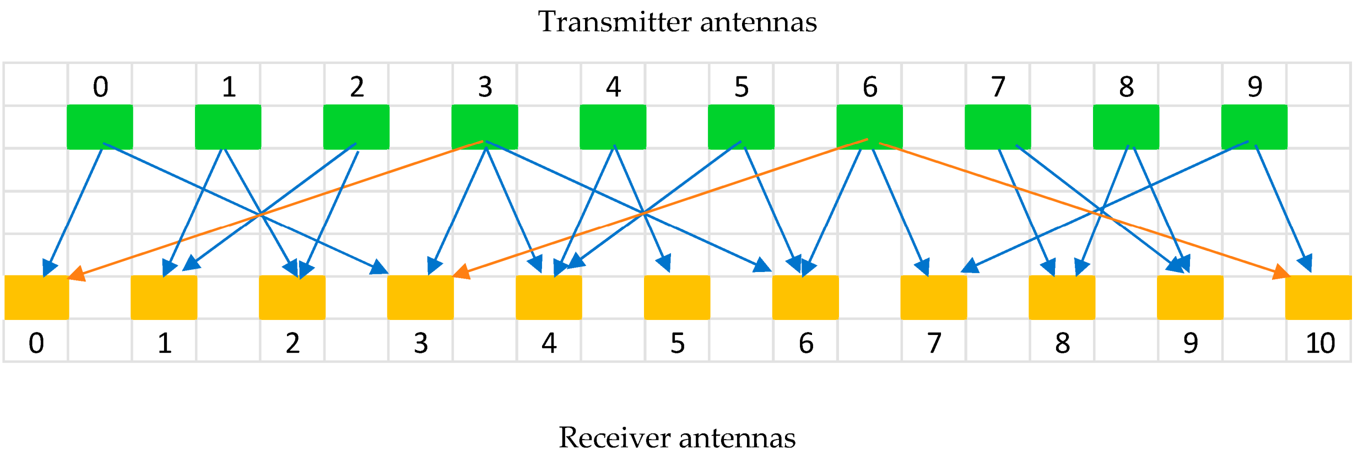

Figure 1. SF-GPR transmitter-receiver antenna pairs.

While the principles of wave propagation and GPR signal interpretation have been widely reported in pertinent GPR references [18–21,25–27], the development of the more than 200 proprietary post-processing algorithms used in the analysis of this system has been presented in past references by the authors [28–30]. The effort required to record, process, analyze, present, and interpret large datasets has been automated with an integrated processing pipeline [29]. The analysis reports are either in tabulated and/or graphical format, as well as GeoTIFF mapping images using GIS. Data collection is assisted with software that provides real-time visual feedback to the field operators about the current coverage and completeness with integrated aerial images. The path of the vehicle using GPS for each data collection pass across the width of the bridge deck is also monitored in real-time. During the development of the automated SF-GPR post-processing analysis, the signal interpretation algorithms were developed for evaluating each one of the key bridge conditions and physical parameters identified and briefly described in a follow-up section. Further details have been presented in past references by the authors [29,30]. To be mentioned that the primary standards currently in place for measuring bridge deck deterioration/delamination are ASTM D 6087-08, "Standard Test Method for Evaluating Asphalt-Covered Bridge Decks Using Ground Penetrating Radar" (also applicable to concrete overlaid decks and concrete decks), and ASTM D4580/D4580M-12 "Standard Practice for Measuring Delamination in Concrete Bridge Decks by Sounding". The developed system satisfies or exceeds the requirements of both ASTM standards in terms of data collection. Moisture effects on EM signal are accounted for with short-time Fourier transform processing, STFT [27]. There are currently 5200 bridges statewide in Maryland, of which approximately 2500 are under the jurisdiction of MD DOT. While further details of the SF-GPR data acquisition system are reported elsewhere [27,28], the speed of data acquisition varies between 12.8 and 72.4 km/h, depending on the selected testing protocol. An optimum speed of acquisition for the proposed system is 16 km/h in order to optimize the data resolution required for each analysis and to minimize loss of accuracy due to surface roughness [30]. An example B-scan for a typical bridge deck profile with three spans and asphalt overlay is shown in Figure 2, while details on the interpretation techniques used in regard to the GPR signal for detecting the bridge deck conditions have been included in a follow-up section.

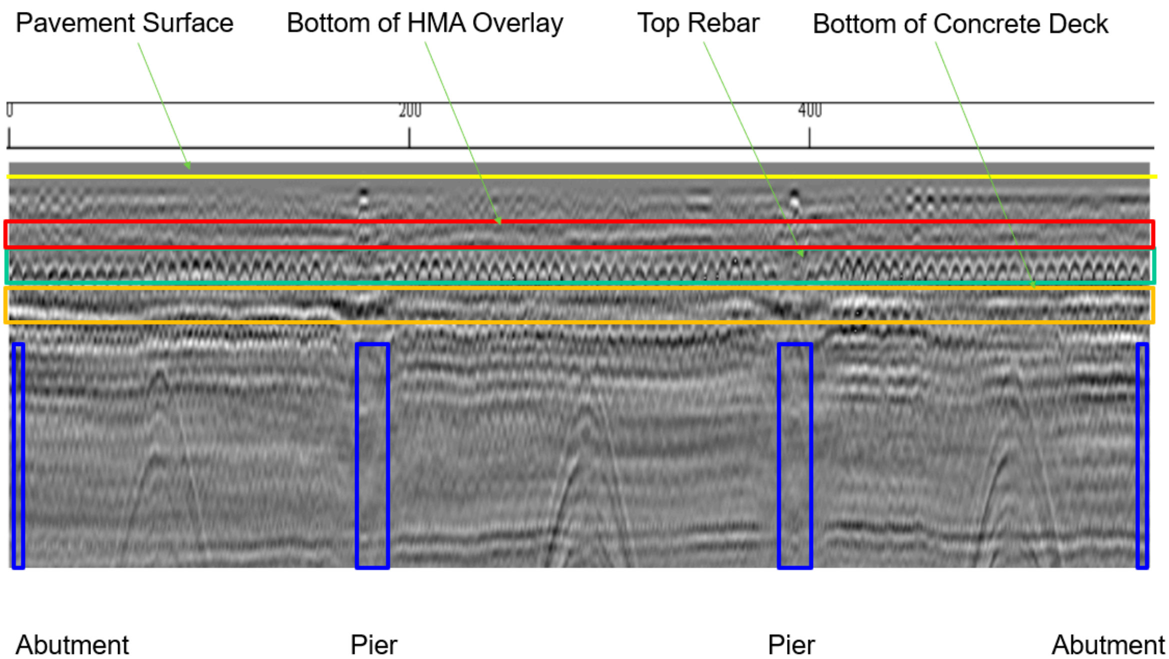

Figure 2. Example Profile View (Bscan of a three-span bridge deck).

The objective of this study was the development of the bridge deck condition rating methodology for the SF-GPR analysis results using fuzzy sets modeling. The fuzzy sets membership functions were defined to reflect the rating score categories considered in the National Bridge Inventory, NBI, database. Thus, the fuzzy sets modeling was built on nine-condition membership functions similar to those NBI rating scale categories. The overall bridge deck condition score leading to each of the nine condition states was based on both bridge deck physical and condition-related parameters obtained from the SF-GPR analysis. Details on the fuzzy set modeling, along with two bridge deck examples, are provided herein.

1.2. Key Bridge Deck Condition Elements from SF-GPR Analysis

The SF-GPR theoretical foundation for signal interpretation algorithms has been developed over the years under Federal Highway Administration (FHWA) sponsored research and included extensive validation and accuracy in relation to "*ground true*" conditions [25,26]. As indicated earlier, in recent years, the need of the Maryland Department of Transportation, MD DOT, to survey thousands of bridge decks in a very short period of time identified the necessity for developing and implementing the processing analysis pipeline system. This need was the result of the federal requirements in reporting and storing every two years the condition of bridge decks in each state in regard to the National Bridge Inventory system [27,28]. This required further development and fine-tuning of hundreds of interpretation and analysis algorithms for transitioning from development to implementation [29,30]. Furthermore, recognizing that the condition rating scores reported in the NBI database are based primarily (i) on subjective and visual ratings of state inspectors and (ii) often reflecting a single or multiple state inspector(s) training and judgment over time, emphasized further the value of NDT-based objective assessment of bridge decks and need to develop a bridge deck rating system to go along such NDT data and analysis. The need for the new rating system has also been reinforced by the feedback of inspectors and bridge engineers reporting that the NBI deck condition values can be within two levels of the scale from the actual condition of the deck [27].

The requirements for higher accuracy data without compromising the speed of data collection identified the need to use a wideband SF-GPR antenna array in near-ground-coupled configuration [29,30]. This also helped to address the agency's requirements of limiting the number of costly lane closures and their safety concerns for both workers and the traveling public and prevented significant travel delays. Such action is necessary when objective measurements are needed from field exploration (i.e., involving coring, chain drag, half-cell potential, and other testing) to: (i) either verify inspector subjective rating or (ii) obtain more accurate condition data.

During the development of the automated SF-GPR post-processing analysis, the signal interpretation algorithms were developed for evaluating each one of the key bridge conditions and physical parameters, presented in Figure 3 and explained next. In contrast, Figure 4 presents the steps of the analysis for achieving the overall condition score fuzzy membership presented in a later section. The key bridge condition assessment elements included: (I) bridge deck "Surface Condition" as a function of surface elevation and concrete surface dielectric, and when applicable, overlay condition; (II) "Rebar Condition" as a function of top rebar cover, dielectric at top of the rebar and signal strength, as well a rebar detection index using rebar presence detection and spacing, and, (III) "Below Rebar Concrete" condition; Both of these last two condition elements constitute an assessment of the bridge deck's "Structural Condition". Based on the above condition elements, the "Overall Score" for the bridge deck condition is obtained (i.e., based on both surface and structural bridge deck condition), Figure 3. These bridge condition assessment elements were assessed based on the following:

- *Concrete Surface Condition (SC):* It is determined based on the variance in material consistency near the surface of the deck using the near-surface dielectric permittivity measured by the GPR sensor. The surface condition is measured using estimates of near-surface dielectric permittivity. It is a function of the amplitude of the first surface reflection in the GPR data and the reference amplitude of the first surface reflection over a metal plate.

- *Surface Elevation (SE):* It is determined based on the vertical deviation from the surface of the deck in centimeters. Depressions (e.g., potholes, cracks) have negative surface elevations, and protrusions (e.g., bumps, overfilled patches) are positive. The vertical distance between the GPR antenna and the surface of the deck is estimated using the first surface reflection. The estimates are calibrated using the common-mid-point method. The surface elevation is computed as a reference height of the GPR antenna with respect to the surface of the deck minus the calibrated vertical distances.
- *Overlay Thickness (OT):* When an HMA or concrete overlay is detected during the pre-processing of the GPR data, its thickness is estimated between the surface and the overlay/concrete-deck interface feature in the GPR measurement. The overlay thickness is reported in centimeters. The thickness of the overlay is estimated as the vertical distance between the surface and the overlay/concrete-deck interface. The estimates of thickness are calibrated using the common-mid-point (CMP) method based on geometric triangulation. Figure 5 shows an example of five lateral offsets of five different transmitter-receiver pairs. Note that all five lines cross at a common midpoint. The distance D2 is estimated using the five measurements, knowing the five lateral offsets. The thickness of the overlay is D2-D1, where D1 is estimated using a similar triangulation.
- *Overlay Condition (OC):* When there is an HMA or concrete overlay detected during the pre-processing of the GPR data, its condition is estimated using the dielectric permittivity near the overlay/concrete-deck interface feature in the GPR measurement and the signal strength of the GPR reflection at the interface. The overlay condition is a dimensionless parameter ranging from 1 (best) to 10 (worst). The condition of the overlay is determined using an estimate of the dielectric permittivity and signal strength of the GPR reflection at/near the overlay/concrete-deck interface. The estimates are computed and calibrated using the common-mid-point method.

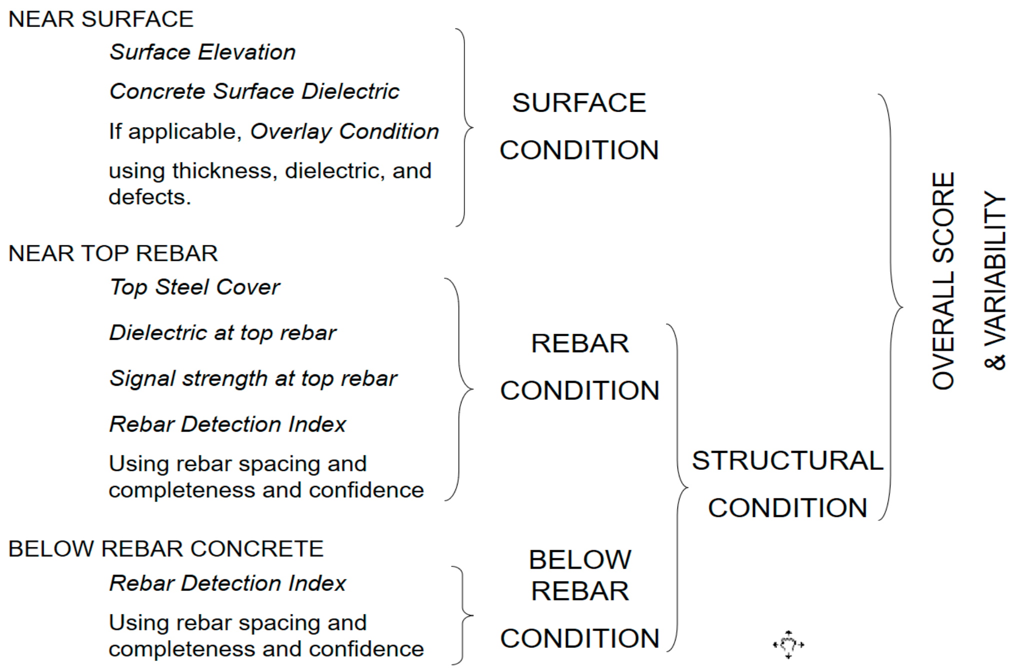

Figure 3. Bridge Deck Condition Assessment Components.

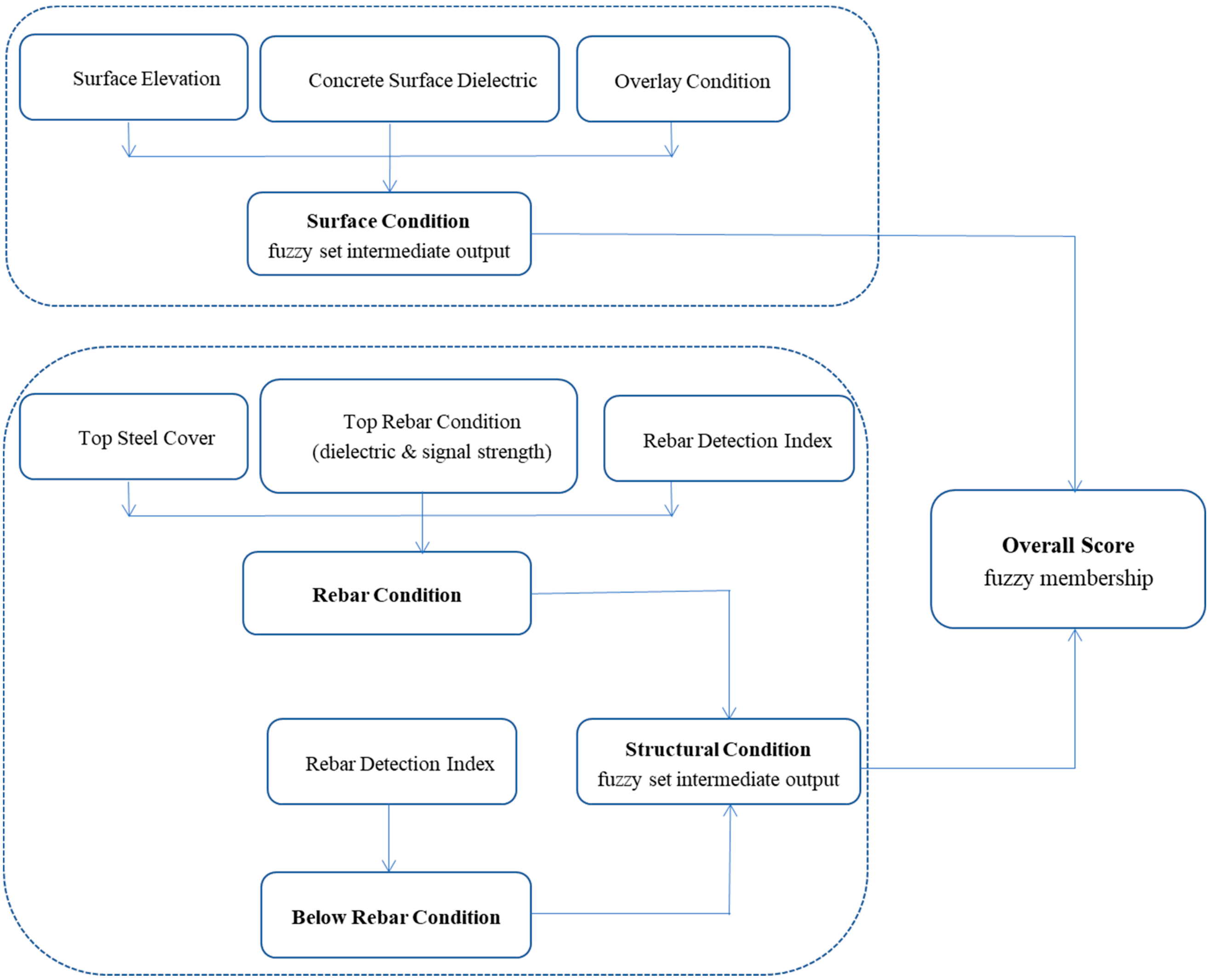

Figure 4. Steps of Analysis for Overall Condition Score Fuzzy Membership.

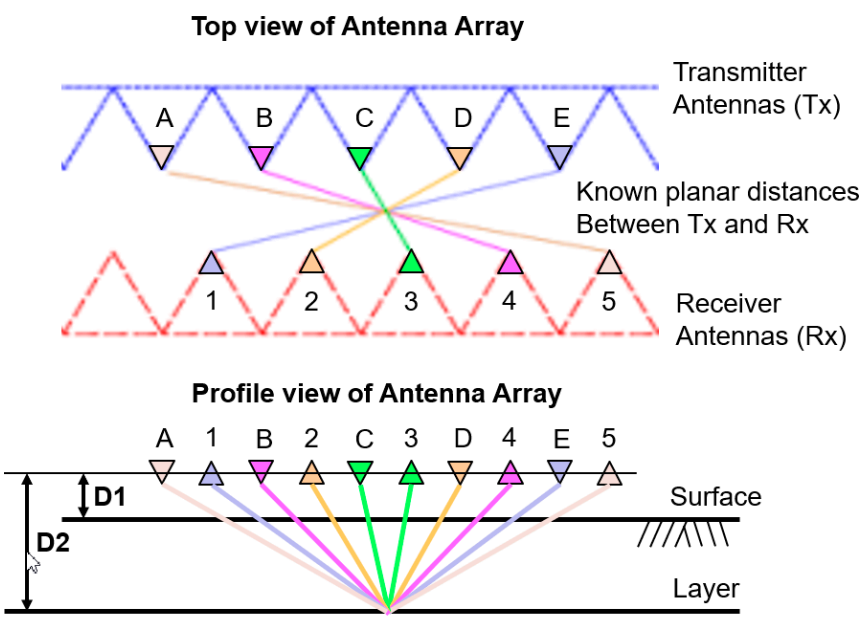

Figure 5. Common-mid-point (CMP) method.

- *Top Steel Cover (TC):* It is determined between the surface and the top steel mat features in the GPR measurement. The top steel cover is reported in centimeters and is estimated as the vertical distance between the surface and the top-steel mat interfaces. The estimates are computed and calibrated using the common-mid-point method.
- *Above Steel Condition (TSC):* It is determined using the dielectric permittivity near the top steel mat interface feature in the GPR measurement and the signal strength of the GPR reflection at the interface. It is a dimensionless parameter ranging from 1 (best) to 10 (worst). The condition of the top steel mat is determined using an estimate of the dielectric permittivity and signal strength of the GPR reflection at/near the top-steel mat interface, at and between the rebars. The estimates are computed and calibrated using the common-mid-point method.
- *Top Steel Condition (ASC):* It is estimated using the dielectric permittivity at the top steel mat interface feature in the GPR measurement and the signal strength of the GPR reflection at the interface. The top steel condition is a dimensionless parameter ranging from 1 (best) to 10 (worst). The estimates are computed and calibrated using the common-mid-point method.
- *Below Steel Condition (BSC):* This is estimated using the dielectric permittivity near the bottom steel mat interface feature in the GPR measurement and the signal strength of the GPR reflection at the interface. The bottom steel condition is a dimensionless parameter ranging from 1 (best) to 10 (worst). The estimates are computed and calibrated using the common-mid-point method.
- *Deck Thickness (DT):* It is determined between the surface and the bottom of the deck interface feature in the GPR measurement. The thickness is reported in centimeters. The estimates are calibrated using the common-mid-point method.
- *Bottom Steel Cover (BC):* It is determined as the vertical distance between the bottom of the deck and the bottom steel mat interface in the GPR measurement. The estimates are computed and calibrated using the common-mid-point method.

2. Fuzzy Sets Condition Rating Modeling

While the "project level" analyses are related to an assessment of each individual condition parameter shown in Figure 3 with details for each bridge deck span, it is the "network-level" analysis that identifies the need for an overall condition score for a bridge deck, as is the case of the NBI rating score, Table 1. Thus, the "network-level results are a synthesis of all detailed information into a master list with overall average scores of such condition parameters for all the spans of a bridge structure. The condition assessment for each bridge deck structure can be computed using the breakdown of each scale into fuzzy sets and the statistics of each distribution. While statistical analysis deal with randomness, fuzzy models attempt to capture and quantify nonrandom imprecision [31]. Thus, the first method to investigate the characteristics of a condition parameter across all structures is to look at the histogram of all structures overlaid onto a single combined histogram plot. Figure 6 shows the combined histogram for Surface Elevation Deviation as an example. The reference histogram was identified from all the available data, shown in bold (red color) in Figure 6a,b. With the reference distribution, the range is represented by the two vertical bold lines at two standard deviations. The process of establishing a reference histogram is repeated for each condition parameter of Figure 3. With the reference range, the next step is to compute the percent area "abnormal" that provides a quantitative measure of the variance for a bridge deck with uniform conditions. Figure 6b shows a sample structure's Surface Elevation Distribution (blue) and Reference Distribution (red) plus the two standard deviation-based Reference Ranges. The resulting "Area Abnormal" outside the Reference Range is shown as a cross-hatched area. This evaluation parameter is computed for structures and for individual spans. The percent area abnormal is equal to:

$$\text{Percent Area Abnormal} = (\text{Area Abnormal} \times \text{Percent Sampling})/\text{Total Area} \quad (1)$$

A second parameter, variability, is computed using a sigmoidal function with an output range of one to five for each structure and for individual spans to quantify the distribution of condition components' localized defects. The input value to the sigmoidal function is a consistency index that is estimated based on the percentage of spans with distribution spread that are significantly different from the overall one. Variability is an indication of the spatial distribution of the pattern on the deck. High variability indicates multiple concentrations of percent area abnormal on the bridge deck that may indicate localized defects and deterioration. Low variability may indicate a pattern spread throughout the bridge deck. This information may be used to select the most effective remediation strategy. For individual spans, the consistency index is directly proportional to the percent abnormal area.

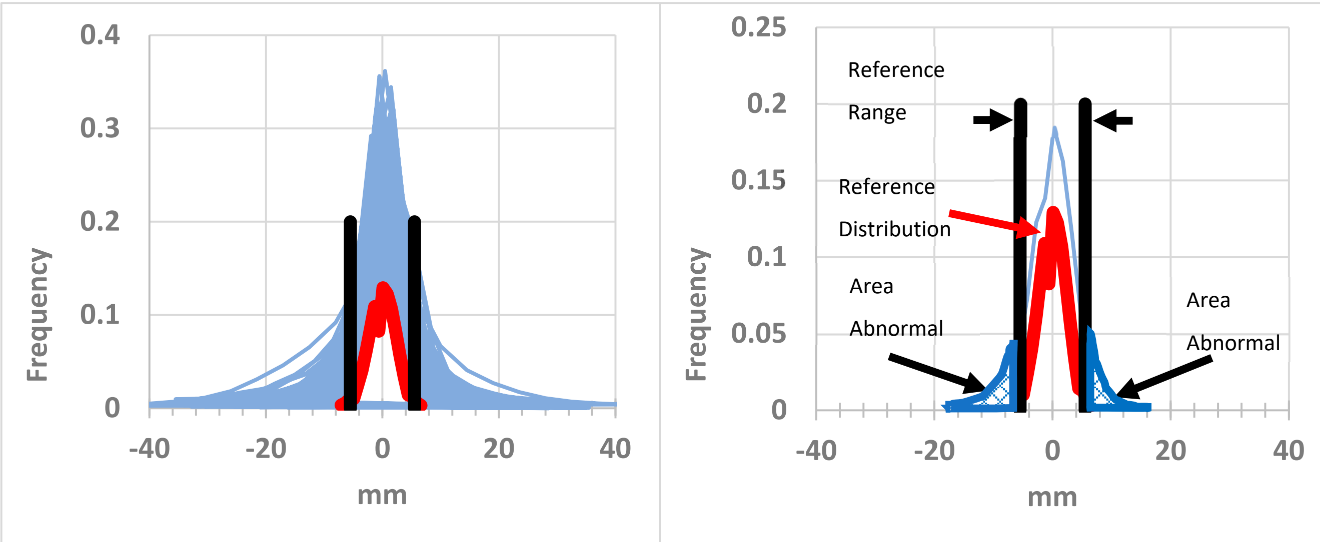

(**a**) (**b**)

Surface Elevation Deviation

Figure 6. Distribution of surface elevation deviation: (**a**) superimposed over the distribution of all bridge decks; (**b**) Range and Distribution (red) histogram for one bridge deck (blue).

Table 1. NBI Condition Rating Scale (adapted from 32).

Rating	Definition	Comments
9	excellent condition	
8	very good condition	no problems noted;
7	good condition	some minor problems;
6	satisfactory condition	structural elements show some minor deterioration;
5	fair condition	all primary structural elements are sound but may have minor section loss, cracking, spalling, or scour;
4	poor condition	advanced section loss, deterioration, spalling, or scour;
3	serious condition	loss of section, deterioration of primary structural elements. Fatigue cracks in steel or shear cracks in concrete may be present;
2	critical condition	advanced deterioration of primary structural elements. Fatigue cracks in steel or shear cracks in concrete may be present, or scouring may have removed substructure support. Unless closely monitored, it may be necessary to close the bridge until corrective action is taken;

Table 1. *Cont.*

Rating	Definition	Comments
1	"imminent" failure condition	major deterioration or section loss present in critical structural components or obvious vertical or horizontal movement affecting structure stability. The bridge is closed to traffic, but corrective action may put it back in light service; and
0	failed condition	out of service and beyond corrective action.

2.1. Fuzzy Sets Architecture

The architecture of fuzzy sets modeling considers the groups of condition parameters that are physically related to the intermediary outputs. For example, the intermediary output "Surface Condition" is a function of "Surface Elevation," "Concrete Surface Dielectric," and, when applicable, "Overlay Condition". Figure 3 shows the case that comprises five components in this fuzzy modeling to produce an overall score and variability: surface condition, rebar condition, below rebar condition, structural condition, and overall score and variability. The parameters of the fuzzy sets establish the contribution of each condition parameter and intermediary output. Each input and output parameter considered in this fuzzy modeling is represented by membership functions, each of which corresponds to a qualitative description of a quantitative level. The analysis process is automated, as presented in Figure 4.

2.2. Fuzzy Sets and NBI Condition Rating Scale

The following case shows how data element #58 [32,33], the "Deck" condition rating of the national bridge inventory (NBI) system, was modeled as a fuzzy set. The "Condition" ratings of the bridge "Deck" provides details of the nature and severity of the defect(s) and are estimated based on inspection reports and analysis of cores. The following codes described in Table 1 provide the definition of the NBI condition ratings scales for data element #58 "Deck" and were used for relating to the nine membership functions (i.e., 1 to 9) in this fuzzy sets modeling.

A fuzzy set comprises three components: the fuzzy function of the fuzzy set and the fuzzy associative memory that relates the data elements to the condition ratings—the output fuzzy set, and if more details are needed, the defuzzification function of the output fuzzy set. For the fuzzy set, i, of each GPR condition element, A_i*, there are m membership functions. In this case, a triangular function was used, Figure 7, to define each membership function i:

$$\mu_{A_j}(x_{ij}) = \begin{cases} 1 - \frac{|\alpha_j - x_{ij}|}{c_j}, & \alpha_j - c_j \le x_{ij} \le \alpha_j + c_j \\ 0, & otherwise \end{cases} \tag{2}$$

where a_j and c_j are the center and half-width of the triangular function, respectively.

For the "Deck" condition rating function, nine membership functions are defined, in Figure 4, as in the case of the nine condition categories in the NBI database scale, Table 1. The centers are 1 through 9, with a half-width of one or less. Figure 7 is a membership function centered at 5 with a width of 1.5. Each membership function is assigned a reference name and a brief description, Table 2 and Figure 8, and are the same as the 9 NBI rating scores of Table 1. In addition to their centers and widths, a label and description parameters are assigned to each membership function. The values in Table 2 are the parameters for the nine membership functions. For example, RE indicates a rating score of 9 for the "excellent" condition, while RF represents a condition score of 5 for the "fair" condition, and so on, for the output deck condition ratings. Figure 8 is a plot of the nine membership functions superimposed. For the edge membership function, the end conditions are set to a constant maximum value of one.

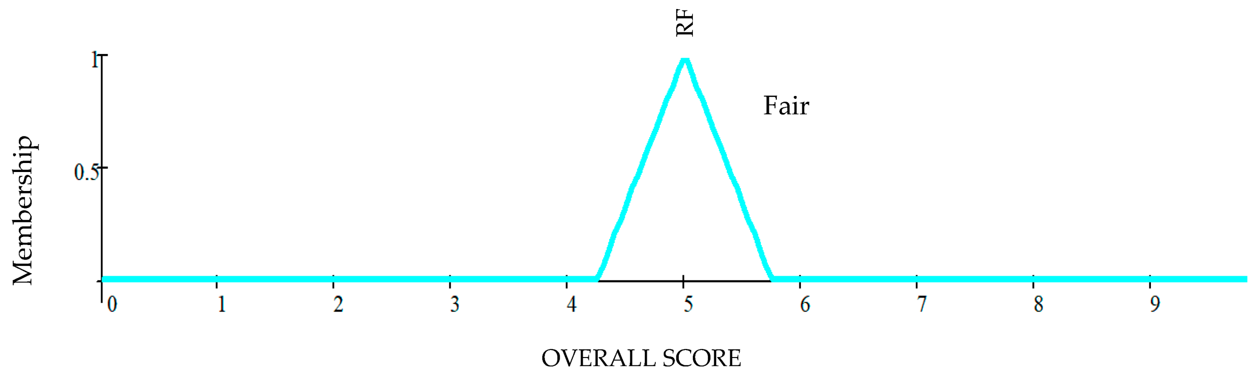

Figure 7. Membership function "RF" for "Fair condition" belonging to output fuzzy set OVERALL SCORE.

Table 2. Parameters for membership functions of output fuzzy set OVERALL SCORE.

Function	RI	RC	RS	RP	RF	RO	RG	RV	RE
Center	1	2	3	4	5	6	7	8	9
Width	2	2	2	2	1.5	1.5	1.5	1.5	2
Description	Imminent Failure	Critical	Serious	Poor	Fair	Satisfactory	Good	Very Good	Excellent

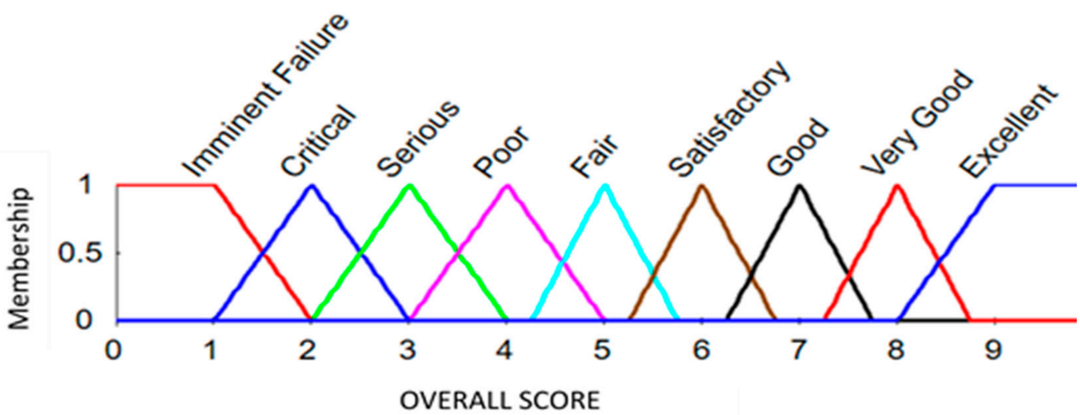

Figure 8. Membership functions of fuzzy set OVERALL SCORE.

3. Example Results and Discussion

In order to demonstrate the proposed fuzzy set modeling developed in this study, a case example of fuzzy computations is presented herein. In this example, two-input (SURFACE CONDITION, SURFACE ELEVATION) and one-output (SURFACE) fuzzy sets are considered, and the results are presented next in Tables 3–7 and Figures 9–11. In detail, Table 3 and Figure 9 present the five membership functions for the SURFACE CONDITION with center values and width for each one. Similarly, Table 4 and Figure 10 present the membership function values for the SURFACE ELEVATION.

The fuzzy associative memory function establishes the correspondence between combinations of input fuzzy sets for the GPR condition parameters and the output fuzzy set, with the SURFACE value equal to:

$$\mu_{out}(X,y) = \begin{cases} k = FAM(X) \\ \mu_A(X) = \operatorname*{Min}_i \left[\mu_{\ A} * (x_i) \right] \\ Min\left[\mu_{\ A}(X), \quad 1 - \frac{|\alpha_k - y|}{c_j} \right] \\ \alpha_k - c_k \le y \ \le \alpha_k + c_k \end{cases} \quad (3)$$

where k is the membership function output by the fuzzy associative memory for the input values X and k corresponding to a condition rating; if there are multiple combinations due to overlap, the final solution is the union of the output fuzzy sets for each combination instead of using the minimum value. The case listed in Table 6 relates the input SURFACE CONDITION and SURFACE ELEVATION DEVIATION to the output fuzzy-set SURFACE. The corresponding membership functions for the output fuzzy-set SURFACE are presented in Table 5 and Figure 11.

The final output value is computed as the centroid of the output fuzzy set:

$$y_c = \frac{\int y\, \mu_{out}(X,y)\, dy}{\int y\, dy} \tag{4}$$

The condition rating can be reported as the centroid value y_c, or as the rating corresponding to the membership function with the largest value at y_c

Table 3. Parameters for membership functions of fuzzy set SURFACE CONDITION.

Function	**SCV**	**SCG**	**SCA**	**SCM**	**SCP**
Center	5	12	20	34	45
Width	11	12	17	19	17
Description	Very Good	Good	Acceptable	Marginal	Poor

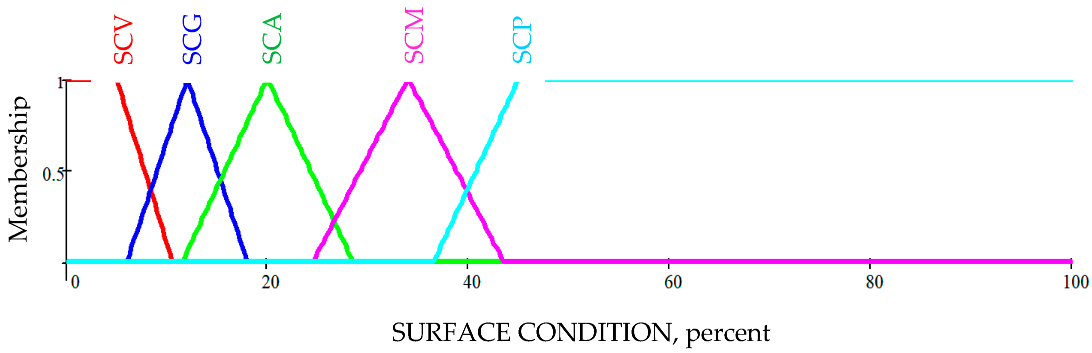

Figure 9. Membership functions of fuzzy set SURFACE CONDITION.

Table 4. Parameters for membership functions of fuzzy set SURFACE ELEVATION.

Function	**SEV**	**SEG**	**SEA**	**SEM**	**SEP**
Center	5	10	17	27	35
Width	8	9	13	14	12
Description	Very Good	Good	Acceptable	Marginal	Poor

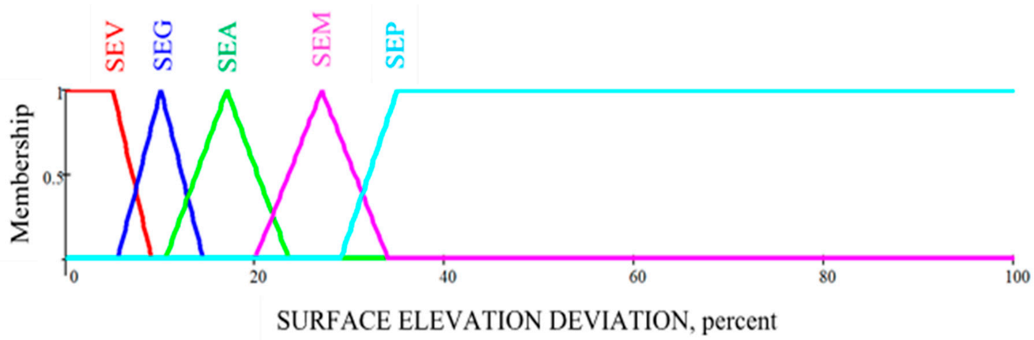

Figure 10. Membership functions of fuzzy set SURFACE ELEVATION DEVIATION.

Table 5. Parameters for membership functions of output fuzzy set SURFACE.

Function	SP	SF	SO	SG	SE
Center	1	3	5	7	9
Width	4	4	4	3	3
Description	Poor Surface	Fair Surface	Satisfactory Surface	Good Surface	Excellent Surface

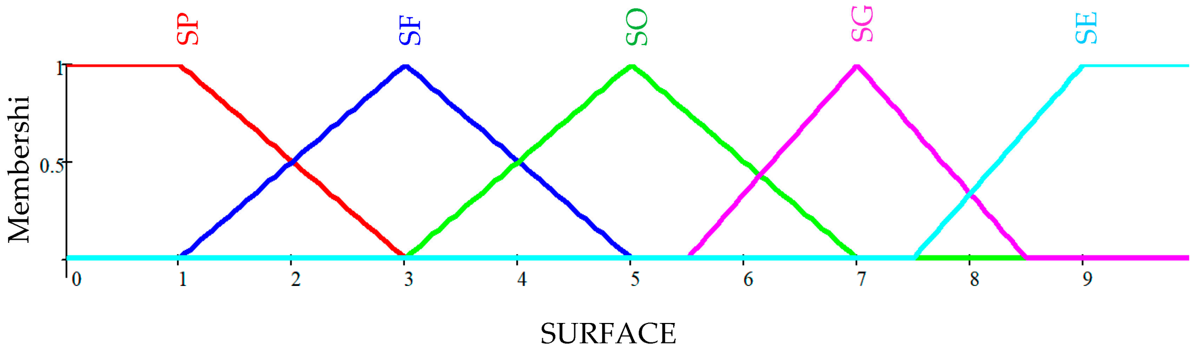

Figure 11. Membership functions of fuzzy set SURFACE.

Table 6. Fuzzy Associative Memory, input SURFACE CONDITION and SURFACE ELEVATION DEVIATION, and output SURFACE.

	SEV	SEG	SEA	SEM	SEP
SCV	SE	SG	SO	SO	SF
SCG	SE	SG	SO	SO	SF
SCA	SG	SG	SO	SF	SP
SCM	SG	SO	SO	SF	SP
SCP	SO	SO	SF	SP	SP

Note: colors reflect membership functions of Figure 8.

In the numerical example included herein, the input condition parameters are presented using such membership functions and fuzzy associative memory. Given an input of 13.5% for SURFACE CONDITION, the two non-zero membership values of 0.75 and 0.235 are computed using Equation (2) for function SCG and SCA, respectively, as shown in Figure 12. This result shows that the input level is mixed between good and acceptable. With 24.5% for SURFACE ELEVATION DEVIATION, the only non-zero membership value of 0.643 is computed using equation 2 for function SEM, as shown in Figure 13. This input level is marginal.

With the example fuzzy associative memory, two input fuzzy-set pairs are presented (SCG/0.75, SEM/0.643) and (SCA/0.235, SEM/0.643), and the output fuzzy-set values are SO/0.643 and SF/0.235, respectively, based on Equation (3) and as shown in Table 7. The yellow highlighted cells of Table 7 represent the results of these two input fuzzy-set pairs (i.e., Case 1 and 2), along with the output from Equation (3) function. Finally, the condition rating is estimated using the defuzzification function in Equation (4). The final defuzzified value for output SURFACE is 4.595 for this case example of one component of the fuzzy model in Figure 14.

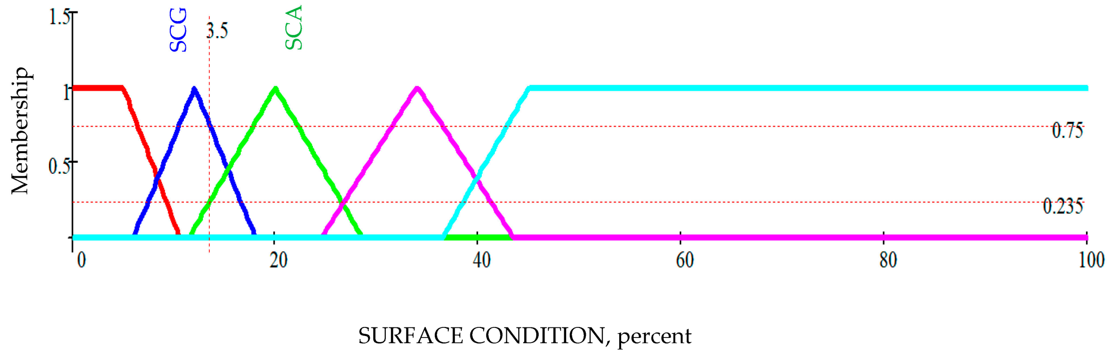

Figure 12. Non-zero membership values for an input value of 13.5% for SURFACE CONDITION.

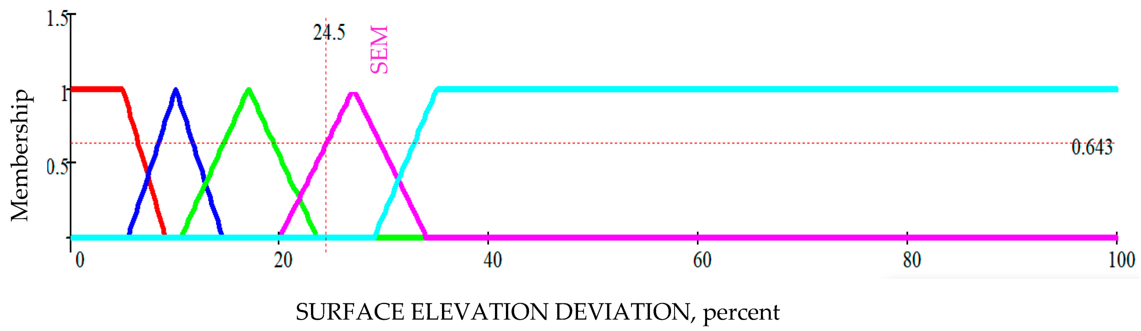

Figure 13. Non-zero membership values for an input value of 24.5% for SURFACE ELEVATION DEVIATION.

Table 7. Estimation of SURFACE using input values and Equation (3).

Case 1: (SCG, SEM)	SEV	SEG	SEA	SEM/0.643	SEP
SCV	SE	SG	SO	SO	SF
SCG/0.75	SE	SG	SO	SO/0.643	SF
SCA	SG	SG	SO	SF	SP
SCM	SG	SO	SO	SF	SP
SCP	SO	SO	SF	SP	SP
Case 2: (SCA, SEM)	SEV	SEG	SEA	SEM/0.643	SEP
SCV	SE	SG	SO	SO	SF
SCG	SE	SG	SO	SO	SF
SCA/0.235	SG	SG	SO	SF/0.235	SP
SCM	SG	SO	SO	SF	SP
SCP	SO	SO	SF	SP	SP

Note: colors reflect membership functions of Figure 8; yellow highlighted cells represent results of the two input fuzzy-set pairs (i.e., Case 1 and 2), along with the output from Equation (3) function.

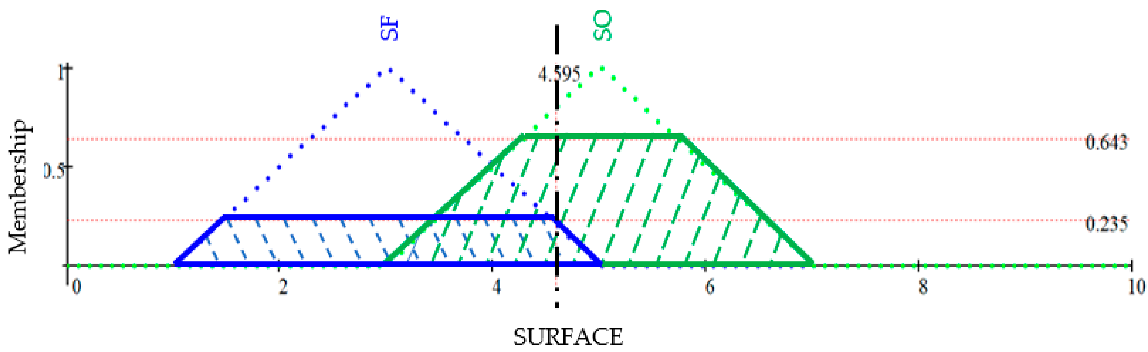

Figure 14. Output values for numerical example.

The analyses of the database are automated, as shown in Figure 4, and are summarized in a master list. Each structure has one record that includes results for all spans and individual spans. The overall score and variability estimated with the fuzzy model and the percentage area abnormal and variability computed for each selected GPR condition parameter are included in the record. Table 8 shows a subset sample of the master list for two of the condition parameters and the overall score. Note that the color coding of each entry provides a quick visual reference of the scores and levels of each parameter. Red is worse; green is better. Colors in-between are indicative of a gradual change from such conditions. A discussion section on how this information can be used follows.

Table 8. Master list with overall scores and variability, percent area abnormal and variability, for two condition parameters.

Description	Span Number	Overall Score	Overall Variability	CSC Surface Condition		SED Surface Elevation Deviation	
				% Area Abnormal	Variability	% Area Abnormal	Variability
Structure 1	0	4.374	2.437	3.016	4.969	31.864	1.031
Structure 1 Span	1	4.371	1.516	7.987	4.210	32.242	1.132
Structure 1 Span	2	4.000	1.181	2.980	1.027	35.908	1.049
Structure 1 Span	3	4.345	1.122	0.897	1.027	32.151	1.027
Structure 1 Span	4	5.000	1.091	1.749	1.300	24.135	1.048
Structure 2	0	3.000	2.156	31.768	3.000	38.892	1.031
Structure 2 Span	1	3.000	1.187	28.409	1.027	37.235	1.027
Structure 2 Span	2	3.000	1.053	30.888	1.027	39.395	1.048
Structure 2 Span	3	3.000	1.568	28.696	4.380	38.431	1.027
Structure 2 Span	4	3.000	1.200	44.706	1.027	41.407	1.048

Note: color variations are indicative of gradual change between the worst (red color) and better (green) conditions. Yellow, orange, light green represent gradual variation in conditions between worst (red color) and better (green) conditions.

While the key components of the fuzzy set analysis were presented with bridge deck case examples, summary results for a select subset group of 169 bridges are summarized next. First, the overall scores for these structures are plotted on a bar chart and in a histogram in Figure 15. The bar chart, Figure 15b, shows the relative variance of the overall score among the structures and individual spans. The histogram shows the relative distribution of the overall scores. In this sample, the dominant score is 5, which describes the condition as "fair." Less than ten percent of the bridges are in "serious" condition.

Second, the information in the master database of all structures can be used to compare individual structures. Table 9 lists the overall scores for two structures and some of the parameters used in the fuzzy-set modeling to estimate them. In this case study, the magnitudes reported for all spans and each individual span are consistent. Also, the variability for this example showed no significant localized inconsistency. Thus, the comparison focused on the magnitudes of each selected condition parameter. In the last column labeled "Global Median", the median values for all structures and spans show that one structure is close to the average condition and the other is lower, confirmed by the overall scores. Such analyses can eventually assist highway engineers in the interpretation of the overall condition assessment of the bridges in the state. When repeated measurements are taken every few years apart, the rate of deterioration and, thus, the impact of maintenance and rehabilitation actions can be analyzed and reported based on such analysis.

While the NBI condition rating categories were used for defining this fuzzy sets modeling, comparison between the two rating scores was not considered since (i) the condition data obtained from the SF-GPR surveys are based on objective evaluation and with EA signal response measurements throughout the bridge deck thickness. As reported previously [27], such measurements are very accurate in relation to the "ground true" conditions since they are based on enhanced data collection protocols and extended post-processing analysis algorithms developed and implemented in SF-GPR, while (ii) the condition scores reported in the NBI database are primarily based on subjective and visual ratings, often reflecting a single or multiple state inspector(s) training and judgment over time; and lastly, (iii) lag in timing between the SF-GPR and state inspector's surveys on the same bridges was in some cases as far as 2.5 to 5 years. As indicated earlier, based on feedback from inspectors and bridge engineers, it is well-accepted that the reported NBI deck condition values can be within two levels of the scale from the actual condition of the deck [30]. For this reason, there is a need for objective measurements (i.e., based on SF-GPR in this case) coupled with a condition rating approach (i.e., in this case, the proposed fuzzy set modeling presented herein). Consequently, such condition rating scores better reflect the actual "ground true" field conditions since they are based on analysis from objective measurements that have already been compared to the ground true conditions [28,29].

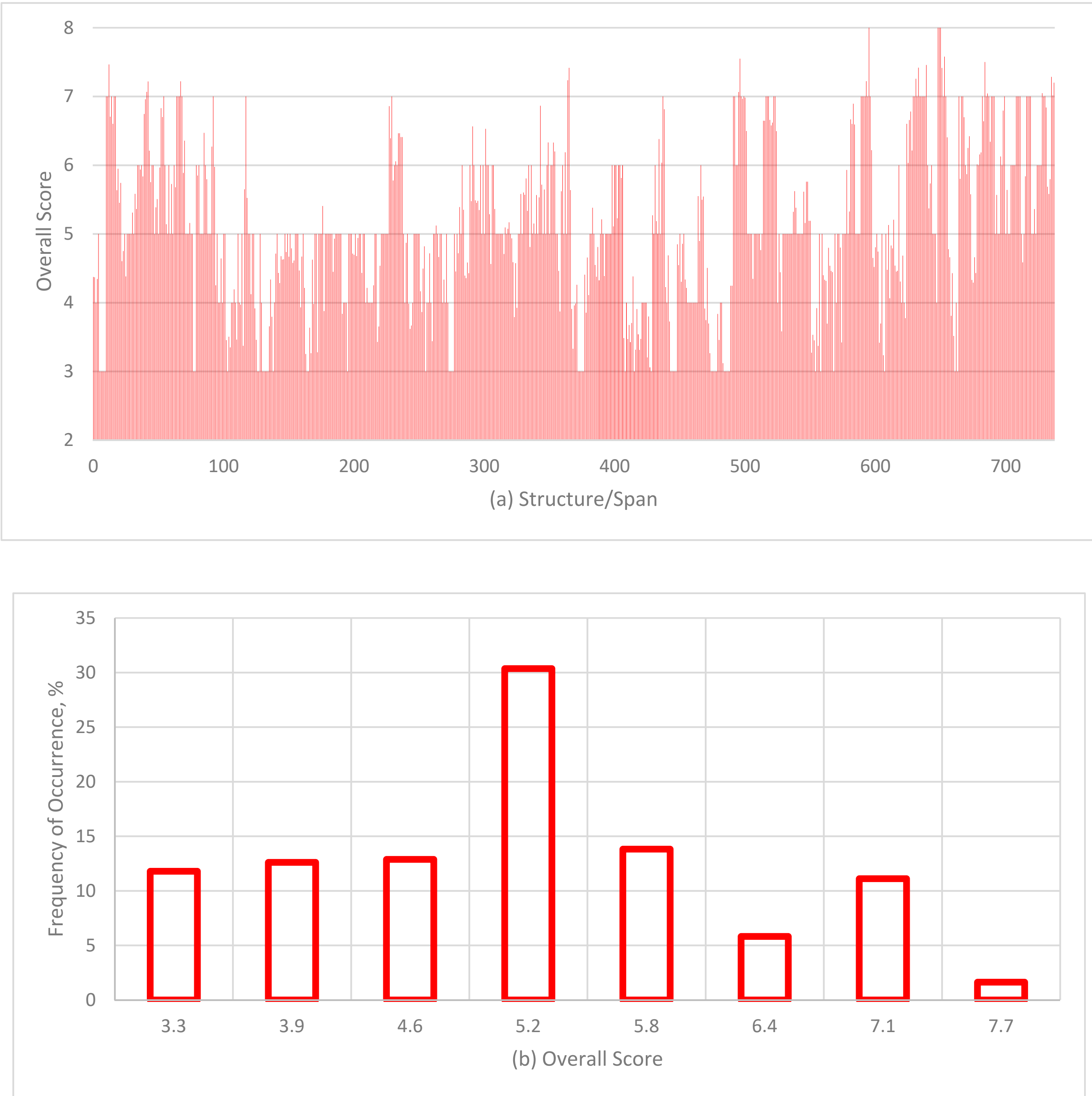

Figure 15. Overall Scores: (**a**) bar chart and (**b**) histogram for 169 structures.

Table 9. Sample of network-level information from master list for two structures.

Structure	Example 1				Example 2				Global
Span	All	1	2	3	All	1	2	3	Median
Overall Score	5.00	5.00	5.00	5.00	3.00	3.00	3.00	3.00	5.00
Surface Condition	7.4	5.4	8.4	7.0	28.9	34.4	26.5	28.1	14.6
Surface Elevation Deviation	21.2	19.5	19.9	25.5	36.1	38.5	34.8	36.2	15.5
Concrete Cover Deviation	13.0	10.2	16.4	8.2	18.9	13.1	20.7	21.1	17.6
Bottom Surface Deviation	21.1	17.2	21.8	23.0	10.6	10.3	10.9	10.3	28.4
Condition at Top Rebar	23.9	19.6	26.0	22.8	9.4	10.2	9.4	8.8	31.4
Condition Above Top Rebar	26.2	24.1	27.6	25.0	7.2	7.5	7.2	6.8	26.0
Condition Between Rebar	6.4	6.2	6.6	6.1	13.3	12.6	13.2	14.1	9.6

4. Summary and Conclusions

SF-GPR provides significant enhancement of bridge deck condition analysis, yet it involves higher complexity in post-processing in regard to other GPR alternatives. Recently an SF-GPR-based system was implemented in Maryland with advanced post-processing algorithms. This system is currently adopted for routine bridge deck surveys. This study explored the development of the bridge deck condition rating methodology using fuzzy sets modeling. The proposed approach defines the condition state from the SF-GPR data using bridge deck physical and condition parameters characterizing "surface condition," "structural condition," and the combined "overall bridge deck score." The proposed novel approach of using fuzzy sets modeling for defining bridge deck condition state was based on nine membership functions reflecting the rating scores reported in NBI. In the proposed fuzzy sets modeling, a second parameter, variability, was introduced to quantify the distribution of the condition parameters in regard to localized defects within a bridge deck or a bridge deck span. In other words, such modeling provides the opportunity to incorporate the spatial distribution of condition patterns within a bridge deck. The definition and interworks of the fuzzy set modeling developed in this study were presented with actual case studies from the database of bridges in the state. These fuzzy sets analyses were integrated into the analysis pipeline of the SF-GPR system in order to provide the current condition assessment rating of individual bridge deck spans, as well as the overall condition rating of the bridge deck structure. The proposed rating approach was developed and implemented for bridge structures in the state.

The developed novel fuzzy sets condition rating approach is able to provide a condition rating of each structure and/or span, as well as comparatively among all surveyed structures in the state. When combined with other sources of information, such as environmental data (annual temperature ranges, freeze cycles, annual rainfall, and snowfall precipitation), traffic volume, and cumulative Equivalent Single Axle Load (ESAL) history, the highway agency can use the analysis to study the factors associated with faster deterioration for some bridge decks. Deck materials and designs may be included as well to investigate their actual performance under a set of given/expected conditions. Prediction models for repair, remediation, or replacement of a bridge deck may be based on the analysis of all bridge decks to improve the criteria for prioritizing, scheduling, or selecting a structure that may need to be more closely monitored because it is likely to deteriorate at a faster rate. Thus, the developed condition rating modeling approach has great promise for multiple purposes in the future and as more bridge SF-GPR surveys are added to the master database for the state. The transferability of this modeling can be explored and validated in other regions where similar bridge deck condition survey practices are considered.

Author Contributions: Conceptualization, N.G., D.G. and J.M.; methodology, NG., D.G. and J.M.; software, N.G. and J.M.; validation, N.G., D.G. and J.M.; writing—original draft preparation, N.G., D.G. and J.M.; writing—review and editing, N.G. and D.G.; funding acquisition, N.G. and D.G. All authors have read and agreed to the published version of the manuscript.

Funding: This research received no external funding.

Data Availability Statement: Data are available upon request to the corresponding author.

Acknowledgments: The authors would like to thank Federal Highway Administration for the support in developing the fundamentals of the analysis of SF-GPR and MD DOT for the development, fine-tuning, and implementation of the SF-GPR analysis.

Conflicts of Interest: The authors declare no conflict of interest.

References

1. FHWA, Bridge Replacement Unit Cost 2020. Available online: https://www.fhwa.dot.gov/bridge/nbi/sd2020.cfm (accessed on 7 April 2022).
2. Hu, D.; Li, S.; Ma, Z.J.; Huang, B. *Concrete Bridge Deck Deterioration Assessment Using Ground Penetrating Radar*; Tennessee DOT RES 2019-17; Department of Civil and Environmental Engineering, The University of Tennessee: Knoxville, TN, USA, 2021.
3. Sun, H.; Pashoutani, S.; Zhu, J. Nondestructive evaluation of concrete bridge decks with automated acoustic scanning system and ground penetrating radar. *Sensors* **2018**, *18*, 1955. [CrossRef] [PubMed]
4. Abu Dabous, S.; Yaghi, S.; Alkass, S.; Moselhi, O. Concrete bridge deck condition assessment using IR Thermography and Ground Penetrating Radar technologies. *Autom. Constr.* **2017**, *81*, 340–354. [CrossRef]
5. Varnavina, A.V.; Sneed, L.H.; Khamzin, A.K.; Torgashov, E.V.; Anderson, N.L. An attempt to describe a relationship between concrete deterioration quantities and bridge deck condition assessment techniques. *J. Appl. Geophys.* **2017**, *142*, 38–48. [CrossRef]
6. Kashif Ur Rehman, S.; Ibrahim, Z.; Memon, S.A.; Jameel, M. Nondestructive test methods for concrete bridges: A review. *Constr. Build. Mater.* **2016**, *107*, 58–86. [CrossRef]
7. Goulias, D.; Cafiso, S.; Di Graziano, A.; Saremi, S.; Currao, V. Condition Assessment of Bridge Decks through Ground Penetration Radar in Bridge Management Systems. *ASCE J. Perform. Constr. Facil.* **2020**, *34*, 04020100. [CrossRef]
8. Dix, C.H. Seismic velocities from surface measurements. *Geophysics* **1955**, *20*, 68–86. [CrossRef]
9. Kee, S.-H.; Fetrat, F.; Gucunski, N. Advanced Signal Interpretation Algorithm for Automated Impact Echo Testing System: Application to Concrete Bridge Decks. In Proceedings of the 91th Annual Transportation Board Meeting, Washington, DC, USA, 22–26 January 2012.
10. Gucunski, N.; Romero, F.; Kruschwitz, S.; Feldmann, R.; Parvardeh, H. *Comprehensive Bridge Deck Deterioration Mapping of Nine Bridges by Nondestructive Evaluation Technologies*; Dept. of Transportation: Ames, IA, USA, 2011.
11. Gucunski, N.; Imani, A.; Romero, F.; Nazarioan, S.; Yuan, D.; Wiggenhauser, H.; Shokouhi, P.; Taffe, A.; Kutrubes, D. *Nondestructive Testing to Identify Concrete Bridge Deck Deterioration*; SHRP S2-R06A-RR-1; Transportation Research Board: Washington, DC, USA, 2013.
12. Abouhamad, M.; Dawood, T.; Jabri, A.; Alsharqawi, M.; Zayed, T. Corrosiveness mapping of bridge decks using image-based analysis of GPR data. *Autom. Constr.* **2017**, *80*, 104–117. [CrossRef]
13. Varnavina, A.V.; Khamzin, A.K.; Torgashov, E.V.; Sneed, L.H.; Goodwin, B.T.; Anderson, N.L. Data acquisition and processing parameters for concrete bridge deck condition assessment using ground-coupled ground penetrating radar: Some considerations. *J. Appl. Geophys.* **2015**, *114*, 123–133. [CrossRef]
14. Alani, A.M.; Aboutalebi, M.; Kilic, G. Applications of ground penetrating radar (GPR) in bridge deck monitoring and assessment. *J. Appl. Geophys.* **2013**, *97*, 45–54. [CrossRef]
15. Sultan, A.A.; Washer, G.A. Reliability Analysis of Ground-Penetrating Radar for the Detection of Subsurface Delamination. *J. Bridg. Eng.* **2018**, *23*, 04017131. [CrossRef]
16. Wang, Z.W.; Zhou, M.; Slabaugh, G.G.; Zhai, J.; Fang, T. Automatic detection of bridge deck condition from ground penetrating radar images. *IEEE Trans. Autom. Sci. Eng.* **2011**, *8*, 633–640. [CrossRef]
17. Barnes, C.L.; Trottier, J.-F. Effectiveness of Ground Penetrating Radar in Predicting Deck Repair Quantities. *J. Infrastruct. Syst.* **2004**, *10*, 69–76. [CrossRef]
18. Al-Qadi, I.; Leng, Z.; Larkin, A. *In-Place Hot Mix Asphalt Density Estimation Using Ground Penetrating Radar*; ICT Report No. 11-096; University of Illinois: Urbana, Champaign, 2011.
19. Scullion, T.; Chen, Y. *Using Ground-Penetrating Radar for Real-Time Quality Control Measurements on New HMA Surfaces*; Research Report 1702-5; Texas Transportation Institute, Texas A&M University: College Station, TX, USA, 1999.
20. Saarenketo, T. *Using Ground-Penetrating Radar and Dielectric Probe Measurements in Pavement Density Quality Control*; Transportation Research Record 1575, TRB; National Research Council: Washington, DC, USA, 1997; pp. 34–41.
21. Maser, K.R.; Scullion, T. *Automated Detection of Pavement Layer Thicknesses and Subsurface Moisture Using Ground Penetrating Radar*; Final Report; Texas Transportation Institute: College Station, TX, USA, 1990.

22. Liu, Z.; Gu, X.; Chen, J.; Wang, D.; Chen, Y.; Wang, L. Automatic recognition of pavement cracks from combined GPR B-scan and C-scan images using multiscale feature fusion deep neural networks. *Autom. Constr.* **2023**, *146*, 104698. [CrossRef]
23. Liu, Z.; Yeoh, J.; Gu, X.; Chen, J.; Dong, Q.; Chen, Y.; Wu, W.; Wang, L.; Wang, D. Automatic pixel-level detection of vertical cracks in asphalt pavement based on GPR investigation and improved mask R-CNN. *Autom. Constr.* **2023**, *146*, 104689. [CrossRef]
24. Omar, T.; Nehdi, M.L.; Zayed, T. Integrated Condition Rating Model for Reinforced Concrete Bridge Decks. *J. Perform. Constr. Facil.* **2017**, *31*. [CrossRef]
25. Gagarin, N.; Mekemson, J. *Non-Destructive Testing of Pavements for Location and Evaluation of In-Roadway Sensor Installations*; Small Business Innovation Research (SBIR) Phase IIb, Program Office, John, A. Volpe National Transportation Systems Center (Volpe Center), U.S. Department of Transportation (DOT): Cambridge, MA, USA, 2011.
26. Starodub, Inc. Travel Way Measurement System. Patent No. US8306747 B1, 6 November 2012.
27. Goulias, D.; Gagarin, N. *Effective Implementation of Ground Penetrating Radar (GPR) for Condition Assessment & Monitoring of Critical Infrastructure Components of Bridges and Highways*; SBIR, Phase 2; Maryland SHA: Hanover, MD, USA, 2016.
28. Goulias, D.; Gagarin, N.; Mekemson, J. Deployment of Step-Frequency (SF) Ground-Penetrating-Radar (GPR) Array System for Condition Assessment of Bridge Decks. In Proceedings of the NDE/NDT for Highways and Bridges: Structural Materials Technology (SMT) 2016, Portland, OR, USA, 29–31 August 2016.
29. Gagarin, N.; Goulias, D.; Mekemson, J.; Cutts, R.; Andrews, J. Development of a Novel Methodology for Assessing Bridge Deck Conditions Using Step Frequency Antenna Array Ground Penetrating Radar. *ASCE J. Perform. Constr. Facil. J.* **2020**, *34*. [CrossRef]
30. Goulias, D. *Optimizing Field Data Collection & Developing Advanced Ground Penetration Radar (GPR) Processing Modules, Phase 3*; Final Research Report, #UM4-54; Maryland State Highway Administration: Hanover, MD, USA, 2020.
31. Zadeh, L.A. Fuzzy Sets. *Inf. Control.* **1965**, *8*, 338–353. [CrossRef]
32. FHWA, National Bridge Inventory, NBI, Updated 5 May 2021. Available online: https://www.fhwa.dot.gov/bridge/nbi.cfm (accessed on 29 January 2023).
33. Saremi, S.; Goulias, D.; Zhao, Y. Alternative Sequence Classification Neural Networks for Bridge Deck Condition Rating. *ASCE J. Perform. Constr. Facil.* **2023**, *37*. [CrossRef]